

Subsampling Sequential Monte Carlo for Static Bayesian Models

David Gunawan^{1,2}, Robert Kohn^{1,2}, Matias Quiroz^{1,2,3},
Khue-Dung Dang^{1,2} and Minh-Ngoc Tran^{2,4}

Abstract

Our article shows how to carry out Bayesian inference by combining data subsampling with Sequential Monte Carlo (SMC). This takes advantage of the attractive properties of SMC for Bayesian computations with the ability of subsampling to tackle big data problems. SMC sequentially updates a cloud of particles through a sequence of densities, beginning with a density that is easy to sample from such as the prior and ending with the posterior density. Each update of the particle cloud consists of three steps: reweighting, resampling, and moving. In the move step, each particle is moved using a Markov kernel and this is typically the most computationally expensive part, particularly when the dataset is large. It is crucial to have an efficient move step to ensure particle diversity. Our article makes two important contributions. First, in order to speed up the SMC computation, we use an approximately unbiased and efficient annealed likelihood estimator based on data subsampling. The subsampling approach is more memory efficient than the corresponding full data SMC, which is a great advantage for parallel computation. Second, we use a Metropolis within Gibbs kernel with two conditional updates. First, a Hamiltonian Monte Carlo update makes distant moves for the model parameters. Second, a block pseudo-marginal proposal is used for the particles corresponding to the auxiliary variables for the data subsampling. We demonstrate the usefulness of the methodology using two large datasets.

Keywords. Hamiltonian Monte Carlo, Large datasets, Likelihood annealing

¹:School of Economics, UNSW Business School, University of New South Wales. ²:ARC Centre of Excellence for Mathematical and Statistical Frontiers (ACEMS). ³:Research Division, Sveriges Riksbank. ⁴:Discipline of Business Analytics, University of Sydney.

1 Introduction

The main aim of Bayesian inference is to obtain the posterior distribution of unknown parameters. Exact simulation approaches such as Markov Chain Monte Carlo (MCMC) (Brooks et al., 2011) methods have been the main methods used for sampling from complex posterior distributions for nearly three decades. Despite this, MCMC methods have some notable drawbacks and limitations. One drawback often overlooked by practitioners when fitting complex models, is the failure to converge caused by poorly mixing chains. While Hamiltonian Monte Carlo (Neal, 2011, HMC) is a remedy in many cases, it can be notoriously difficult to tune. Limitations of MCMC methods include the difficulty of assessing convergence, the difficulty of parallelizing the computation and the difficulty of estimating the marginal likelihood efficiently from MCMC output, the latter being useful for model selection (Kass and Raftery, 1995). Sequential Monte Carlo (see Doucet et al., 2001 for an introductory overview) methods provide an alternative exact simulation approach to MCMC methods and overcome some of their drawback. Moreover, in contrast to MCMC methods, SMC can provide online updates of the parameters, which is particularly useful for dynamic (time-varying parameters) models. However, SMC is also useful for static (non time-varying parameters) models (Chopin, 2002; Del Moral et al., 2006), and can in such cases more easily explore multimodal posterior distributions than MCMC.

Despite the advantages of SMC, it is remarkably less used than MCMC for static models. One possible explanation is that, while amenable to computer parallelization, it is still very computationally expensive and particularly so for large datasets. Another obstacle caused by large datasets is that they prevent efficient computer parallelization of SMC, as the full dataset needs to be available for each worker which is infeasible as it consumes too much Random-Access Memory (RAM). We propose an efficient data subsampling approach which significantly reduces both the computational cost of the algorithm and the memory requirements when parallelizing; see Section 3.6 for a detailed explanation of the latter. Our approach utilizes methods previously developed for Subsampling MCMC (Quiroz et al., 2018; Dang et al., 2017) and places them within the SMC framework.

In a Bayesian context, SMC is a method to traverse a cloud of particles through a sequence of distributions, with the initial distribution both easy to sample from and to evaluate, while the final distribution is the posterior distribution. For each distribution in the sequence, the cloud of particles is an estimate of the distribution. The particles consist of the unknown parameters and any additional latent variables that are part of the model. The evolution of the particle cloud consists of three steps:

reweighting, resampling and moving. Of these, the first two steps are common to all SMC schemes and are straightforward. The move step is the most expensive and is critical to ensure that the particle cloud is representative of the distribution it aims to estimate.

To the best of our knowledge, data subsampling has not been explored in SMC for static models. We consider a likelihood annealing approach in which we estimate the annealed likelihood efficiently using an approximately unbiased estimator. Likelihood estimates for SMC in a non-subsampling context have been used in Duan and Fulop (2015), who propose to estimate the likelihood unbiasedly using a particle filter in a time series state space model application. However, Duan and Fulop (2015) use a random walk MCMC kernel for the move step of the model parameters, which is inefficient in high dimensions and we now turn to this issue.

The literature has focused on accelerating SMC algorithms by designing efficient MCMC kernels for the move step to achieve efficient particle diversity. The efficiency concept here is the ability of the MCMC kernel to generate distant proposals which have a high probability of being accepted, so as to move the particle efficiently using as few iterations of the kernel as possible. Various approaches exist to achieve this. For example, adaptive SMC adapts the tuning parameters of the kernel to improve its efficiency (Jasra et al., 2011; Fearnhead and Taylor, 2013). A different approach is explored in South et al. (2016), who use SMC with a flexible independent proposal based on copulas models. Finally, the use of derivatives to construct efficient proposals through the Metropolis Adjusted Langevin Algorithm (Roberts and Stramer, 2002, MALA) have been explored (Sim et al., 2012; South et al., 2017). It is now well-known that MALA is a special case of the more general proposal utilizing Hamiltonian dynamics proposed in Duane et al. (1987) (see Neal 2011; Betancourt 2017 for introductory overviews). Although South et al. (2017) mention HMC in their introduction, they only consider MALA in their paper and show how neural networks can be applied to adaptively choose its tuning parameters. Daviet (2016) considers HMC proposals for particle diversity, however, HMC is painfully slow for very large datasets and therefore this approach does not scale well in the number of data observations.

We propose data subsampling to improve the computational efficiency and a HMC type of kernel for efficient particle diversity, while leveraging on data subsampling in order to achieve scalability in the number of observations. As a by-product, data subsampling lowers the memory requirements of the algorithm (see Section 3.6), making it amenable for computer parallelism on very large datasets. Our framework combines that of Duan and Fulop (2015) for carrying out SMC with an estimated likelihood, Quiroz et al. (2018) for estimating the likelihood and controlling the error

in the target density and Dang et al. (2017) for constructing efficient proposals for high-dimensional targets in a subsampling context.

Our article is organized as follows. Section 2 reviews sequential Monte Carlo for static models. Section 3 outlines our methodology, which scales SMC to large datasets and high-dimensional models by combining efficient data subsampling and Hamiltonian Monte Carlo to sample from an accurate approximate target density. Section 4 applies our methodology to two large datasets and shows that it gives accurate estimates of both the posterior density and the marginal likelihood. Section 5 concludes.

2 Sequential Monte Carlo

2.1 SMC for static Bayesian models

Denote the observed data $\mathbf{y} = (\mathbf{y}_1^\top, \dots, \mathbf{y}_n^\top)^\top$, with $\mathbf{y}_k \in \mathcal{Y} \subset \mathbb{R}^{d_y}$. Let $\boldsymbol{\theta}$ be the vector of unknown parameters, such that $\boldsymbol{\theta} \in \Theta \subset \mathbb{R}^{d_\theta}$, with $p(\boldsymbol{\theta})$ and $p(\mathbf{y}|\boldsymbol{\theta})$ the prior and likelihood. In Bayesian inference, the uncertainty about the unobserved $\boldsymbol{\theta}$ is specified by the posterior density $\pi(\boldsymbol{\theta})$, which by Bayes' theorem is

$$\pi(\boldsymbol{\theta}) = \frac{p(\boldsymbol{\theta})p(\mathbf{y}|\boldsymbol{\theta})}{p(\mathbf{y})}, \quad \text{where} \quad p(\mathbf{y}) = \int_{\Theta} p(\mathbf{y}|\boldsymbol{\theta}) p(\boldsymbol{\theta}) d\boldsymbol{\theta}, \quad (1)$$

is the marginal likelihood, also known as the evidence, and is often used for Bayesian model selection.

An important aim of Bayesian inference is to estimate the posterior expectation of a function of $\boldsymbol{\theta}$,

$$\mathbb{E}_\pi(\varphi) = \int_{\Theta} \varphi(\boldsymbol{\theta}) \pi(\boldsymbol{\theta}) d\boldsymbol{\theta}. \quad (2)$$

In simulation based inference, this is typically achieved by sampling from (1) and computing (2) by Monte Carlo integration. A second aim is to compute $p(\mathbf{y})$ in (1). However, it is well-known that standard Monte Carlo integration is very inefficient for this task.

In a Bayesian context, SMC (Doucet et al., 2001) is a collection of methods that can sample from (1) and in addition provide an efficient estimate of the marginal likelihood. Their early use was for inference in dynamic systems (Liu and Chen, 1998; Gilks and Berzuini, 2001), but more recently their potential has been realized for static (non-dynamic) models (Chopin, 2002; Del Moral et al., 2006), in which they generalize importance sampling approaches such as Annealed Importance Sampling (Neal, 2001, AIS).

SMC specifies a sequence of P densities, connecting the density of the prior $p(\boldsymbol{\theta})$ to the density of the posterior $\pi(\boldsymbol{\theta})$ in (1). The sequence is usually obtained either through data annealing (Chopin, 2002), in which the data is introduced sequentially, or temperature annealing (Neal, 2001), in which the likelihood is tempered $p(\mathbf{y}|\boldsymbol{\theta})^{a_p}$ with $a_0 = 0 < a_1 < \dots < a_P = 1$. Our article considers the latter and we note at the outset that we propose to estimate the tempered likelihood by data subsampling; see Section 3. The tempered posterior is

$$\pi_p(\boldsymbol{\theta}) = \frac{\eta_p(\boldsymbol{\theta})}{Z_p}, \text{ where } \eta_p(\boldsymbol{\theta}) = p(\mathbf{y}|\boldsymbol{\theta})^{a_p} p(\boldsymbol{\theta}) \quad \text{and} \quad Z_p = \int_{\Theta} p(\mathbf{y}|\boldsymbol{\theta})^{a_p} p(\boldsymbol{\theta}) d\boldsymbol{\theta}. \quad (3)$$

SMC proceeds by sampling a set of M particles from the prior $p(\boldsymbol{\theta})$ and traverses them through the sequence of densities $\pi_p(\boldsymbol{\theta}), p = 1, \dots, P$, for each p , by (i) reweighting, (ii) resampling and (iii) moving the particles. At the final $p = P$, the (weighted) particles are a sample from $\pi(\boldsymbol{\theta})$. We now discuss this in more detail.

The initial particle cloud $\{\boldsymbol{\theta}_{1:M}^{(0)}, W_{1:M}^{(0)}\}$ is obtained by generating the $\{\boldsymbol{\theta}_{1:M}^{(0)}\}$ from $p(\boldsymbol{\theta})$, and giving them equal weight, i.e., $W_{1:M}^{(0)} = 1/M$. The weighted particles $\{\boldsymbol{\theta}_{1:M}^{(p-1)}, W_{1:M}^{(p-1)}\}$ at the $(p-1)$ st stage, $p = 1, \dots, P$, are samples from $\pi_{p-1}(\boldsymbol{\theta})$. At the p th stage, the transition from $\pi_{p-1}(\boldsymbol{\theta})$ to $\pi_p(\boldsymbol{\theta})$ is obtained by the *reweighting step*,

$$w_i^{(p)} = W_i^{(p-1)} \frac{\eta_p(\boldsymbol{\theta}_i^{(p-1)})}{\eta_{p-1}(\boldsymbol{\theta}_i^{(p-1)})} = W_i^{(p-1)} p(\mathbf{y}|\boldsymbol{\theta}_i^{(p-1)})^{a_p - a_{p-1}},$$

and then normalizing $W_i^{(p)} = w_i^{(p)} / \sum_{i'=1}^M w_{i'}^{(p)}$. The reweighting will, when p increases, assign vanishingly smaller weights to particles which are unlikely under the tempered likelihood, causing the so-called particle degeneracy problem, in which the weight mass is concentrated only on a small fraction of the particles, causing a small effective sample size (explained in Section 2.2). This is resolved by the *resampling step*, in which the particles $\boldsymbol{\theta}_{1:M}^{(p)}$ are sampled with a probability equal to their weights $W_{1:M}^{(p)}$, and subsequently setting $W_{1:M}^{(p)} = 1/M$. While this ensures that particles with a small weights are eliminated, it causes so-called particle depletion because the particles with large weights may duplicate. This is resolved by the *move step*, in which an invariant Markov kernel K_p is applied to each of the particles to move them R steps. Notice that since a particle at stage p is distributed as $\pi_p(\boldsymbol{\theta})$ and, moreover, K_p is invariant, there is no burn-in period as in MCMC methods, where possibly a very large number of burn-in iterations are required. Finally, we note that the algorithm is easy to parallelize with respect to the particle dimension, because the computations required for each particle do not depend on that of the other particles. Thus, provided that $p(\mathbf{y}|\boldsymbol{\theta})$ can be computed at each worker without storage issues,

it is straightforward to implement the parallel version.

Del Moral et al. (2006) provide consistency results for estimating (2) based on SMC output and a central limit theorem.

2.2 Statistical efficiency of SMC

The statistical efficiency of the p th stage of the SMC reweighting part is measured through the Effective Sample Size (ESS) defined as

$$\text{ESS}_p = \left(\sum_{i=1}^M \left(W_i^{(p)} \right)^2 \right)^{-1}.$$

The ESS varies between 1 and M , where a low value of ESS indicates that the weights are concentrated only on a few particles. A common problem in SMC is the choice of tempering sequence $\{a_p, p = 1, \dots, P\}$, which has a substantial impact on ESS and therefore needs careful choice. We follow Del Moral et al. (2012) and choose the tempering sequence adaptively to ensure a sufficient level of particle diversity by selecting the next value of a_p such that ESS stays close to some target value $\text{ESS}_{\text{target}}$. We do so by evaluating the ESS over a grid points $a_{1:G,p}$ of potential values of a_p for a given p and select a_p as that value of $a_{g,p}$, $g = 1, \dots, G$, whose ESS is closest to $\text{ESS}_{\text{target}}$.

For this adaptive choice of tempering sequence, Beskos et al. (2016) consider consistency results for estimating (2) based on SMC output and provides a central limit theorem.

2.3 Marginal likelihood estimation with SMC

The marginal likelihood $p(\mathbf{y})$ is often used in the Bayesian literature to compare models by their posterior model probabilities (Kass and Raftery, 1995). An advantage of SMC is that it automatically produces an estimate $p(\mathbf{y})$.

Using the notation of Section 2.1, we note that $p(\mathbf{y}) = Z_P$ and $Z_0 = 1$, so that

$$p(\mathbf{y}) = \prod_{p=1}^P \frac{Z_p}{Z_{p-1}} \quad \text{with} \quad \frac{Z_p}{Z_{p-1}} = \int \left(\frac{\eta_p(\boldsymbol{\theta})}{\eta_{p-1}(\boldsymbol{\theta})} \right) \pi_{p-1}(\boldsymbol{\theta}) d\boldsymbol{\theta}.$$

Because the particle cloud $\left\{ \boldsymbol{\theta}_{1:M}^{(p-1)}, W_{1:M}^{(p-1)} \right\}$ at the $(p-1)$ st stage is a sample from

$\pi_{p-1}(\boldsymbol{\theta})$, the ratio above is estimated by

$$\frac{\widehat{Z_{a_p}}}{Z_{a_{p-1}}} = \sum_{i=1}^M W_i^{(p-1)} \frac{\eta_p(\boldsymbol{\theta}_i^{(p-1)})}{\eta_{p-1}(\boldsymbol{\theta}_i^{(p-1)})}.$$

The estimate of the marginal likelihood is then

$$\widehat{p}(\mathbf{y}) = \prod_{p=1}^P \frac{\widehat{Z_{a_p}}}{Z_{a_{p-1}}}. \quad (4)$$

3 Methodology

3.1 Sequence of target densities

Suppose that $\mathbf{y} = (y_k, k = 1, \dots, n)$ are independent given $\boldsymbol{\theta}$ so that the likelihood and log-likelihood can be written as

$$L(\boldsymbol{\theta}) = \prod_{k=1}^n p(y_k|\boldsymbol{\theta}) \quad \text{and} \quad \ell(\boldsymbol{\theta}) = \sum_{k=1}^n \ell_k(\boldsymbol{\theta}), \quad (5)$$

where $\ell_k(\boldsymbol{\theta}) = \log p(y_k|\boldsymbol{\theta})$. We are concerned with the case where the log-likelihood is computationally very costly, because n is so large that repeatedly computing this sum is impractical.

Quiroz et al. (2018) propose to subsample m observations and estimate $\ell(\boldsymbol{\theta})$ by $\widehat{\ell}_m(\boldsymbol{\theta})$ in (8) and subsequently estimate $L(\boldsymbol{\theta})$ by

$$\widehat{L}(\boldsymbol{\theta}) = \exp\left(\widehat{\ell}_m(\boldsymbol{\theta}) - \frac{1}{2}\widehat{\sigma}_m^2(\boldsymbol{\theta})\right), \quad (6)$$

where $\widehat{\sigma}_m^2(\boldsymbol{\theta})$ is an estimate of $\sigma^2(\boldsymbol{\theta}) = \mathbb{V}(\widehat{\ell}_m(\boldsymbol{\theta}))$. The motivation for (6) is that $\exp(\widehat{\ell}_m(\boldsymbol{\theta}) - \sigma^2(\boldsymbol{\theta})/2)$ is unbiased for $L(\boldsymbol{\theta})$ when $\widehat{\ell}_m(\boldsymbol{\theta})$ is normal. Otherwise, if it is not normal or if the variance $\sigma^2(\boldsymbol{\theta})$ is estimated, it is unbiased for a perturbed likelihood $L_{(m,n)}(\boldsymbol{\theta})$. Quiroz et al. (2018) show that when using the control variate in Section 3.2 in the estimator $\widehat{\ell}_m(\boldsymbol{\theta})$, the fractional error of the perturbed likelihood is

$$\left| \frac{L_{(m,n)}(\boldsymbol{\theta}) - L(\boldsymbol{\theta})}{L(\boldsymbol{\theta})} \right| = \mathcal{O}\left(\frac{1}{nm^2}\right).$$

Our approach is based on extending the target at the p th density, i.e. $\pi_p(\boldsymbol{\theta})$ in (3), to include the set of subsampling indices $\mathbf{u} = (u_1, \dots, u_m)$, where $\mathbf{u} \in \mathcal{U} \subset \{1, \dots, n\}^m$ when sampling data observations with replacement. The extended target

at the p th density is

$$\bar{\pi}_p(\boldsymbol{\theta}, \mathbf{u}) \propto \left(\widehat{L}(\boldsymbol{\theta})\right)^{a_p} p(\boldsymbol{\theta}) p(\mathbf{u}) = \left(\exp\left(\widehat{\ell}_m(\boldsymbol{\theta}) - \frac{1}{2}\widehat{\sigma}_m^2(\boldsymbol{\theta})\right)\right)^{a_p} p(\boldsymbol{\theta}) p(\mathbf{u}), \quad (7)$$

where $p(\mathbf{u})$ is the density of \mathbf{u} (or, more strictly, a probability mass function since \mathbf{u} is discrete). At the final annealing step, (7) becomes $\bar{\pi}_P(\boldsymbol{\theta}, \mathbf{u}) \propto \widehat{L}(\boldsymbol{\theta}) p(\boldsymbol{\theta}) p(\mathbf{u})$, which is the target considered in Quiroz et al. (2018). Quiroz et al. (2018) show that the perturbed marginal density for $\boldsymbol{\theta}$, $\pi_{(m,n)}(\boldsymbol{\theta}) = \int_{\mathbf{u}} \bar{\pi}_P(\boldsymbol{\theta}, \mathbf{u}) d\mathbf{u}$ converges in the total variation metric to $\pi(\boldsymbol{\theta})$ at the rate $\mathcal{O}(1/(nm^2))$. Hence, our proposed approach is approximate but can be very accurate while also scaling well with respect to the subsample size. For example, if we take $m = \mathcal{O}(\sqrt{n})$, then by Quiroz et al. (2018, Part (i) of Theorem 1)

$$\int_{\Theta} |\pi_{(m,n)}(\boldsymbol{\theta}) - \pi(\boldsymbol{\theta})| d\boldsymbol{\theta} = \mathcal{O}\left(\frac{1}{n^2}\right).$$

Moreover, suppose that $\varphi(\boldsymbol{\theta})$ is a scalar function such that $\limsup \mathbb{E}_{\pi}(\varphi^2(\boldsymbol{\theta})) < \infty$. Then, by Quiroz et al. (2018, Part (ii) of Theorem 1)

$$\left| \mathbb{E}_{\pi_{(m,n)}}(\varphi(\boldsymbol{\theta})) - \mathbb{E}_{\pi}(\varphi(\boldsymbol{\theta})) \right| = \mathcal{O}\left(\frac{1}{n^2}\right).$$

This gives our algorithm the theoretical guarantees of converging at a very fast rate to the truth as n increases, both with respect to the density (as measured by total variation) and with respect to the posterior moments. We confirm empirically that we get very accurate inference in our application in Section 4, even for a very small m relative to n .

The next section describes the approach in Quiroz et al. (2018) for obtaining efficient estimators of the log-likelihood. Section 3.3 describes the reweighting and resampling steps. Section 3.4 describes the Markov move step. Section 3.5 shows how to estimate the marginal likelihood. Finally, Section 3.6 outlines the memory advantage of our method for parallel computation compared to standard (non-subsampling) SMC. Algorithm 3 summarizes our approach.

3.2 Efficient estimator of the log-likelihood

Quiroz et al. (2018) propose to estimate $\ell(\boldsymbol{\theta})$ in (5) by the unbiased difference esti-

mator,

$$\widehat{\ell}_m(\boldsymbol{\theta}) = \sum_{k=1}^n q_k(\boldsymbol{\theta}) + \frac{n}{m} \sum_{i=1}^m \ell_{u_j}(\boldsymbol{\theta}) - q_{u_j}(\boldsymbol{\theta}), \quad u_j \in \{1, \dots, n\} \text{ iid}, \quad (8)$$

where

$$\Pr(u_j = k) = \frac{1}{n} \text{ for all } k = 1, \dots, n \text{ and } j = 1, \dots, m,$$

and $q_k(\boldsymbol{\theta}) \approx \ell_k(\boldsymbol{\theta})$ are control variates. The estimator is based on writing

$$\ell(\boldsymbol{\theta}) = \sum_{k=1}^n q_k(\boldsymbol{\theta}) + \sum_{k=1}^n d_k(\boldsymbol{\theta}) = q(\boldsymbol{\theta}) + d(\boldsymbol{\theta}),$$

with $d_k(\boldsymbol{\theta}) = \ell_k(\boldsymbol{\theta}) - q_k(\boldsymbol{\theta})$, $q(\boldsymbol{\theta}) = \sum_k q_k(\boldsymbol{\theta})$, and $d(\boldsymbol{\theta}) = \sum_k d_k(\boldsymbol{\theta})$. The right term in (8) is an unbiased estimate of $d(\boldsymbol{\theta})$. We now discuss a choice of control variates due to Bardenet et al. (2017), which computes $q(\boldsymbol{\theta})$ in $\mathcal{O}(1)$ time. Hence, the cost of computing the estimator is $\mathcal{O}(m)$ and we can take $m = \mathcal{O}(\sqrt{n})$ in order to achieve the convergence rates $\mathcal{O}(1/n^2)$ for both the perturbed density and its moments as discussed in Section 3.1.

Let $\bar{\boldsymbol{\theta}}$ be some posterior location estimate of $\boldsymbol{\theta}$, for example the mean, obtained from a current particle cloud from $\bar{\pi}_p(\boldsymbol{\theta}, \mathbf{u})$. A second order Taylor series expansion of the log-density around $\bar{\boldsymbol{\theta}}$ is

$$\ell_k(\boldsymbol{\theta}) = \ell_k(\bar{\boldsymbol{\theta}}) + \nabla_{\boldsymbol{\theta}} \ell_k(\bar{\boldsymbol{\theta}})^\top (\boldsymbol{\theta} - \bar{\boldsymbol{\theta}}) + \frac{1}{2} (\boldsymbol{\theta} - \bar{\boldsymbol{\theta}})^\top (\nabla_{\boldsymbol{\theta}\boldsymbol{\theta}^\top}^2 \ell_k(\bar{\boldsymbol{\theta}})) (\boldsymbol{\theta} - \bar{\boldsymbol{\theta}}) + o(\|\boldsymbol{\theta} - \bar{\boldsymbol{\theta}}\|),$$

and we therefore approximate $\ell_k(\boldsymbol{\theta})$ by

$$q_k(\boldsymbol{\theta}) = \ell_k(\bar{\boldsymbol{\theta}}) + \nabla_{\boldsymbol{\theta}} \ell_k(\bar{\boldsymbol{\theta}})^\top (\boldsymbol{\theta} - \bar{\boldsymbol{\theta}}) + \frac{1}{2} (\boldsymbol{\theta} - \bar{\boldsymbol{\theta}})^\top (\nabla_{\boldsymbol{\theta}\boldsymbol{\theta}^\top}^2 \ell_k(\bar{\boldsymbol{\theta}})) (\boldsymbol{\theta} - \bar{\boldsymbol{\theta}}),$$

and $o(\delta)$ denotes the small order of δ , meaning $o(\delta)/\delta \rightarrow 0$ as $\delta \rightarrow 0$. Then,

$$q(\boldsymbol{\theta}) = A(\bar{\boldsymbol{\theta}}) + B(\bar{\boldsymbol{\theta}}) (\boldsymbol{\theta} - \bar{\boldsymbol{\theta}}) + \frac{1}{2} (\boldsymbol{\theta} - \bar{\boldsymbol{\theta}})^\top C(\bar{\boldsymbol{\theta}}) (\boldsymbol{\theta} - \bar{\boldsymbol{\theta}}),$$

where

$$A(\bar{\boldsymbol{\theta}}) = \sum_k \ell_k(\bar{\boldsymbol{\theta}}), B(\bar{\boldsymbol{\theta}}) = \sum_k \nabla_{\boldsymbol{\theta}} \ell_k(\bar{\boldsymbol{\theta}})^\top \text{ and } C(\bar{\boldsymbol{\theta}}) = \sum_k \nabla_{\boldsymbol{\theta}\boldsymbol{\theta}^\top}^2 \ell_k(\bar{\boldsymbol{\theta}}).$$

Note that the sums $A(\bar{\boldsymbol{\theta}})$, $B(\bar{\boldsymbol{\theta}})$, and $C(\bar{\boldsymbol{\theta}})$ are computed only once at every stage of the SMC, regardless of the number of particles. Then, for each particle, estimating $d(\boldsymbol{\theta})$ by $\widehat{d}_m(\boldsymbol{\theta}) = (n/m) \sum_j d_{u_j}(\boldsymbol{\theta})$ is computed in $\mathcal{O}(m)$ time and so is (8) because

$q(\boldsymbol{\theta})$ is $\mathcal{O}(1)$. Finally, we can estimate $\sigma^2(\boldsymbol{\theta}) = \mathbb{V}(\widehat{\ell}_m(\boldsymbol{\theta}))$ by

$$\widehat{\sigma}_m^2(\boldsymbol{\theta}) = \frac{n^2}{m^2} \sum_{j=1}^m (d_{u_j}(\boldsymbol{\theta}) - \bar{d}_{\mathbf{u}}(\boldsymbol{\theta}))^2,$$

where $\bar{d}_{\mathbf{u}}(\boldsymbol{\theta})$ denotes the mean of the d_{u_j} for the sample $\mathbf{u} = (u_1, \dots, u_m)$. We note that $\widehat{\sigma}_m^2(\boldsymbol{\theta})$ comes at virtually no cost since it involves terms that are already evaluated when computing $\widehat{d}_m(\boldsymbol{\theta})$.

3.3 The reweighting and resampling steps

The initial particle cloud is now $\{\boldsymbol{\theta}_{1:M}^{(0)}, \mathbf{u}_{1:M}^{(0)}, W_{1:M}^{(0)}\}$, obtained by generating the $\{\boldsymbol{\theta}_{1:M}^{(0)}, \mathbf{u}_{1:M}^{(0)}\}$ from $p(\boldsymbol{\theta})$ and $p(\mathbf{u})$, and assigning equal weights, i.e., $W_{1:M}^{(0)} = 1/M$. The weighted particles $\{\boldsymbol{\theta}_{1:M}^{(p-1)}, \mathbf{u}_{1:M}^{(p-1)}, W_{1:M}^{(p-1)}\}$ at the $(p-1)$ st stage are a sample from $\bar{\pi}_{p-1}(\boldsymbol{\theta}, \mathbf{u})$ and are propagated to $\bar{\pi}_p(\boldsymbol{\theta}, \mathbf{u})$, by updating the weights

$$W_{1:M}^{(p)} = \frac{w_{1:M}^{(p)}}{\sum_{i=1}^M w_i^{(p)}}, \text{ where } w_i^{(p)} = W_i^{(p-1)} \left(\exp \left(\widehat{\ell}_m(\boldsymbol{\theta}_i^{(p-1)}) - \frac{1}{2} \widehat{\sigma}_m^2(\boldsymbol{\theta}_i^{(p-1)}) \right) \right)^{a_p - a_{p-1}}.$$

The resampling step is described in Section 2.1.

3.4 The Markov move step

We now outline the Markov move step of our approach, which utilizes Hamiltonian dynamics to propose distant particle moves and data subsampling in order to efficiently compute the dynamics. Similarly to Section 2.1, the Markov move is designed to leave each of the sequence target densities $\bar{\pi}_p(\boldsymbol{\theta}, \mathbf{u})$, for $p = 0, \dots, P$ invariant. To accommodate subsampling, it is divided into two parts and is described in Algorithm 1.

Algorithm 1 Single Markov move with a kernel invariant for $\bar{\pi}_p(\boldsymbol{\theta}, \mathbf{u})$ in (7).

For $i = 1, \dots, M$,

1. Sample $\mathbf{u}_i | \boldsymbol{\theta}_i, \mathbf{y}$: Propose $\mathbf{u}^* \sim p(\mathbf{u})$, and set $\mathbf{u}_i = \mathbf{u}^*$, with probability

$$\alpha_{\mathbf{u}} = \min \left(1, r := \frac{\exp \left(\widehat{\ell}_m(\boldsymbol{\theta}_i, \mathbf{u}^*) - \frac{1}{2} \widehat{\sigma}_m^2(\boldsymbol{\theta}_i, \mathbf{u}^*) \right)^{a_p}}{\exp \left(\widehat{\ell}_m(\boldsymbol{\theta}_i, \mathbf{u}_i) - \frac{1}{2} \widehat{\sigma}_m^2(\boldsymbol{\theta}_i, \mathbf{u}_i) \right)^{a_p}} \right), \quad (9)$$

The \mathbf{u}^* is proposed from the prior and is independent of the current value of \mathbf{u}_i , so the difference between the log of the numerator and log of the denominator of the ratio r in (9) can be highly variable. This step might get stuck when the numerator is significantly overestimated. A remedy is to induce a high correlation ρ between the log of the estimated annealed likelihood at the current and proposed draws in (9). This can be achieved either through correlating the \mathbf{u} as in Deligiannidis et al. (2017) (see Quiroz et al. 2018 for discrete \mathbf{u}) or by block updates of \mathbf{u} as in Tran et al. (2017). We implement the block updates of Tran et al. (2017) with G blocks, which gives a correlation $\rho \approx 1 - \frac{1}{G}$.

2. Sample $\boldsymbol{\theta}_i | \mathbf{u}_i, \mathbf{y}$: Given a subset of data \mathbf{u}_i , we move the particle $\boldsymbol{\theta}_i$ using a Hamiltonian Monte Carlo (HMC) proposal in a Metropolis-Hastings (MH) algorithm. This becomes a standard HMC move for a given subset \mathbf{u} .

Note that the above is a Gibbs update of $\boldsymbol{\theta}_i, \mathbf{u}_i | \mathbf{y}$. The MH within Gibbs performed in Step 1. is valid (Johnson et al., 2013) and so is the HMC within Gibbs (Neal, 2011) in Step 2. Therefore, this kernel has $\bar{\pi}_p(\boldsymbol{\theta}, \mathbf{u})$ as its invariant distribution. Dang et al. (2017) previously proposed an MCMC version of this algorithm.

We now discuss the HMC proposal to sample a continuous high-dimensional parameter $\boldsymbol{\theta}$ from its full conditional posterior density, for which we use the notation $p(\boldsymbol{\theta} | \text{rest})$. See Neal (2011) for an introductory overview and Betancourt (2017) for a conceptual introduction with an emphasis of its ability to explore high-dimensional spaces.

HMC generates distant proposals that have a high acceptance probability. It therefore avoids the slow exploration of the parameter space typically encountered in random walk proposals, especially in high dimensions. Suppose we wish to sample $\boldsymbol{\theta} \in \Theta \subset \mathbb{R}^{d_\theta}$ from a density proportional to $\exp(\mathcal{L}(\boldsymbol{\theta}))$, where

$$\mathcal{L}(\boldsymbol{\theta}) = \log p(\boldsymbol{\theta} | \text{rest}), \quad (10)$$

is the logarithm of the full conditional posterior density of $\boldsymbol{\theta}$ (up to a normalizing constant). HMC augments the density in (10) with an auxiliary momentum vector \mathbf{r} having the same dimension as $\boldsymbol{\theta}$, with the density $p(\mathbf{r}) = \mathcal{N}(\mathbf{r} | 0, \mathbf{M})$, where \mathbf{M}

is a mass matrix and $\mathcal{N}(\cdot|\boldsymbol{\mu}, \boldsymbol{\Sigma})$ denotes the multivariate normal density with mean vector $\boldsymbol{\mu}$ and covariance matrix $\boldsymbol{\Sigma}$. We define the joint conditional density of $(\boldsymbol{\theta}, \mathbf{r})$ as

$$p(\boldsymbol{\theta}, \mathbf{r}|\text{rest}) \propto \exp(-\mathcal{H}(\boldsymbol{\theta}, \mathbf{r})), \quad (11)$$

where $\mathcal{H}(\boldsymbol{\theta}, \mathbf{r}) = -\mathcal{L}(\boldsymbol{\theta}) + \frac{1}{2}\mathbf{r}^\top \mathbf{M}^{-1}\mathbf{r}$ is called the Hamiltonian. HMC samples from the joint density (11) by utilizing Hamilton's equations, which give a law of motion for the parameters $\boldsymbol{\theta}$ and the momentum variables \mathbf{r} in continuous time,

$$\frac{d\boldsymbol{\theta}}{dt} = \frac{\partial \mathcal{H}}{\partial \mathbf{r}} = \mathbf{M}^{-1}\mathbf{r}, \quad \frac{d\mathbf{r}}{dt} = -\frac{\partial \mathcal{H}}{\partial \boldsymbol{\theta}} = \nabla_{\boldsymbol{\theta}}\mathcal{L}(\boldsymbol{\theta}), \quad (12)$$

where $\nabla_{\boldsymbol{\theta}}$ denotes the gradient with respect to $\boldsymbol{\theta}$. The Hamiltonian \mathcal{H} has important properties such as reversibility, energy conservation and volume preservation (Neal, 2011). Energy conservation means that $d\mathcal{H}/dt = 0$ and hence, if we move according to the dynamics in (12), \mathcal{H} maintains a constant value. By generating a Metropolis-Hastings proposal this way, we end up with the same value of \mathcal{H} at the current and proposed, leading to an acceptance probability of one. However, this is an idealized situation as the dynamics can only be analytically solved for trivial cases and in practice one resorts to discretization methods that approximately conserve energy which we now discuss.

Discretization methods use a small step size ϵ to approximate the continuous dynamics in (12). The ‘‘leapfrog’’ integrator is a popular method where one step of the dynamics is approximated by

$$\begin{aligned} \mathbf{r}\left(t + \frac{\epsilon}{2}\right) &= \mathbf{r}(t) + \epsilon \nabla_{\boldsymbol{\theta}}\mathcal{L}(\boldsymbol{\theta}(t)) / 2 \\ \boldsymbol{\theta}(t + \epsilon) &= \boldsymbol{\theta}(t) + \epsilon \mathbf{M}^{-1}\mathbf{r}\left(t + \frac{\epsilon}{2}\right) \\ \mathbf{r}(t + \epsilon) &= \mathbf{r}(t + \epsilon/2) + \epsilon \nabla_{\boldsymbol{\theta}}\mathcal{L}(\boldsymbol{\theta}(t + \epsilon)) / 2. \end{aligned}$$

The leapfrog integrator provides a mapping $(\boldsymbol{\theta}, \mathbf{r}) \rightarrow (\boldsymbol{\theta}^*, \mathbf{r}^*)$ that is both time-reversible and volume preserving (Neal, 2011). It follows that the Metropolis-Hastings algorithm with acceptance probability

$$\min\left(1, \frac{\exp\left(\mathcal{L}(\boldsymbol{\theta}^*) - \frac{1}{2}\mathbf{r}^{*T}\mathbf{M}^{-1}\mathbf{r}^*\right)}{\exp\left(\mathcal{L}(\boldsymbol{\theta}) - \frac{1}{2}\mathbf{r}^\top\mathbf{M}^{-1}\mathbf{r}\right)}\right)$$

produces an ergodic, time-reversible Markov chain that satisfies detailed balance and whose stationary density for $\boldsymbol{\theta}$ is $p(\boldsymbol{\theta}|\text{rest})$ (Liu, 2001; Neal, 1996). Algorithm 2 summarizes the HMC algorithm.

The performance of HMC depends strongly on choosing suitable values for the mass matrix \mathbf{M} , the step size ϵ , and the number of leapfrog steps L . The step size ϵ determines how well the leapfrog integration approximates the continuous Hamiltonian dynamics in (12). If ϵ is too large, then HMC gives an acceptance rate that is too low as the energy conservation property deteriorates due to a poor approximation. Conversely, if it is too small, then it becomes computationally expensive to obtain distant proposals because a large L is necessary. If L is too large, in addition to being computationally expensive, HMC might generate proposals that retrace their steps. On the other hand, if L is too small, the proposal will be close to the current value, resulting in undesirable random walk behavior. Our article adopts an adaptive method based on Garthwaite et al. (2015) to select ϵ such that it yields a pre-specified average acceptance probability $\bar{\alpha}$ across all particles. In our applications in Section 4, we set $L = 10$, $\bar{\alpha} = 0.8$ and takes the mass matrix $\mathbf{M} = \Sigma^{-1}(\bar{\boldsymbol{\theta}})$, which is the negative Hessian of the log posterior evaluated at $\bar{\boldsymbol{\theta}}$. The mass matrix is computed using the full dataset once for each of the target densities $\bar{\pi}_p(\boldsymbol{\theta}, \mathbf{u})$.

Algorithm 2 Hamiltonian Monte Carlo

Given initial values of $\boldsymbol{\theta}$, ϵ , L , where L is the number of leapfrog updates

Sample $\mathbf{r} \sim \mathcal{N}(\mathbf{0}, \mathbf{M})$

For $l = 1$ to L

Set $(\boldsymbol{\theta}^*, \mathbf{r}^*) \leftarrow \text{Leapfrog}(\boldsymbol{\theta}, \mathbf{r}, \epsilon)$

end for

With probability $\alpha = \min\left(1, \frac{\exp(\mathcal{L}(\boldsymbol{\theta}^*) - \frac{1}{2}\mathbf{r}^{*T}\mathbf{M}^{-1}\mathbf{r}^*)}{\exp(\mathcal{L}(\boldsymbol{\theta}) - \frac{1}{2}\mathbf{r}^T\mathbf{M}^{-1}\mathbf{r})}\right)$, then set $\boldsymbol{\theta} = \boldsymbol{\theta}^*$, $\mathbf{r}^* = -\mathbf{r}$.

Algorithm 3 Subsampling Sequential Monte Carlo

1. Initially, sample the particles $\{\boldsymbol{\theta}_i^{(0)}, \mathbf{u}_i^{(0)}\}$ from the prior densities $p(\boldsymbol{\theta})$ and $p(\mathbf{u})$ and give all particles equal weights, $W_i = 1/M$, $i = 1, \dots, M$. Initialize $p = 0$.
2. While the tempering sequence $a_p \neq 1$ do
 - (a) Set $p \leftarrow p + 1$
 - (b) Find a_p adaptively to maintain the ESS around $\text{ESS}_{\text{target}}$ (Section 2.2).
 - (c) Reweighting: compute the unnormalized weights

$$\begin{aligned}
 w_i^{(p)} &= W_i^{(p-1)} \frac{\eta_{a_p}(\boldsymbol{\theta}_i^{(p-1)}, \mathbf{u}_i^{(p-1)})}{\eta_{a_{p-1}}(\boldsymbol{\theta}_i^{(p-1)}, \mathbf{u}_i^{(p-1)})} \\
 &= W_i^{(p-1)} \left(\exp \left(\widehat{\ell}_m(\boldsymbol{\theta}_i^{(p-1)}) - \frac{1}{2} \widehat{\sigma}_m^2(\boldsymbol{\theta}_i^{(p-1)}) \right) \right)^{a_p - a_{p-1}},
 \end{aligned}$$

and normalize as $W_i^{(p)} = \frac{w_i}{\sum_{i'=1}^M w_{i'}}$, $i = 1, \dots, M$.

- (d) Compute $\bar{\boldsymbol{\theta}}$ as $\bar{\boldsymbol{\theta}} = \sum_{i=1}^M W_i^{(p)} \boldsymbol{\theta}_i^{(p-1)}$ and then obtain

$$\sum_{k=1}^n \ell_k(\bar{\boldsymbol{\theta}}), \quad \sum_{k=1}^n \nabla_{\boldsymbol{\theta}} \ell_k(\bar{\boldsymbol{\theta}}), \quad \sum_{k=1}^n \nabla_{\boldsymbol{\theta}\boldsymbol{\theta}^\top}^2 \ell_k(\bar{\boldsymbol{\theta}})$$

and the mass matrix $\mathbf{M} = \boldsymbol{\Sigma}^{-1}(\bar{\boldsymbol{\theta}})$. Note that this step is based on the full dataset.

- (e) Resample the particles $\{\boldsymbol{\theta}_i^{(p-1)}, \mathbf{u}_i^{(p-1)}\}_{i=1}^M$ using the weights $\{W_i^{(p)}\}_{i=1}^M$ to obtain resampled particles $\{\boldsymbol{\theta}_i^{(p)}, \mathbf{u}_i^{(p)}\}_{i=1}^M$ and set $W_i^{(p)} = 1/M$.
 - (f) Apply R Markov moves to each particle $\boldsymbol{\theta}_i^{(p)}, \mathbf{u}_i^{(p)}$ using Algorithm 1.
-

3.5 Estimating the Marginal Likelihood

Our approach can naturally be extended from Section 2.3 by considering the augmented target density $\bar{\pi}_p(\boldsymbol{\theta}, \mathbf{u})$ in (7). Specifically, $\{\boldsymbol{\theta}_{1:M}^{(p-1)}, \mathbf{u}_{1:M}^{(p-1)}, W_{1:M}^{(p-1)}\}$ at the $(p-1)$ st sequence is a sample from $\bar{\pi}_{a_{p-1}}(\boldsymbol{\theta}, \mathbf{u})$, and hence we estimate the ratio Z_p/Z_{p-1} by

$$\frac{\widehat{Z}_p}{Z_{p-1}} = \sum_{i=1}^M W_i^{(p-1)} \frac{\eta_p(\boldsymbol{\theta}_i^{(p-1)}, \mathbf{u}_i^{(p-1)})}{\eta_{p-1}(\boldsymbol{\theta}_i^{(p-1)}, \mathbf{u}_i^{(p-1)})},$$

and the marginal likelihood estimate is obtained using this expression in (4).

3.6 Efficient memory management by data subsampling

We now explain in detail how data subsampling helps parallel computing from a memory point of view. Suppose first that we perform standard SMC (using all the data) and that we apply computer parallelism using N workers, so that each worker deals with M/N particles (on average). In this case, for each stage p , the computations performed for each particle require repeated likelihood evaluations (using all n data) when applying R move steps with the Markov kernel. Hence, each worker needs to have access to the full dataset.

Suppose now that we use our data subsampling approach in the same setting using M/N particles for each of the N workers. Then, at the beginning of each stage p of the algorithm, we still require a full data evaluation for computing $A(\bar{\boldsymbol{\theta}})$, $B(\bar{\boldsymbol{\theta}})$ and $C(\bar{\boldsymbol{\theta}})$ in Section 3.2. However, at each p , we can now subsample the data according to $\mathbf{u}_i^{(p-1)}$ for each particle and subsequently perform the R move steps with the Markov kernel, which now require repeated estimated likelihood evaluations (using $m \ll n$ observations) and in addition $A(\bar{\boldsymbol{\theta}})$, $B(\bar{\boldsymbol{\theta}})$ and $C(\bar{\boldsymbol{\theta}})$. Now each worker needs to have access only to the subsampled dataset, as well as $A(\bar{\boldsymbol{\theta}})$, $B(\bar{\boldsymbol{\theta}})$ and $C(\bar{\boldsymbol{\theta}})$. However, these are only summaries of the full dataset and are therefore very memory efficient.

Finally, we note that this procedure still requires loading the full dataset into memory. In cases when this is not possible, the MapReduce programming model (Dean and Ghemawat, 2008) can be explored. See Gunawan et al. (2017) for an implementation of MapReduce for the difference estimator.

4 Application

4.1 Models and data

We illustrate our methodology on a logistic regression model and also carry out model selection for two different datasets. The model for the response $y_i \in \{0, 1\}$ given a set of covariates $\mathbf{x}_i \in \mathbb{R}^{d_x}$ and parameters $\boldsymbol{\theta} \in \mathbb{R}^{d_\theta}$, with $d_x = d_\theta$, is

$$p(y_i|\mathbf{x}_i, \boldsymbol{\theta}) = \left(\frac{1}{1 + \exp(\mathbf{x}_i^\top \boldsymbol{\theta})} \right)^{y_i} \left(\frac{1}{1 + \exp(-\mathbf{x}_i^\top \boldsymbol{\theta})} \right)^{1-y_i}. \quad (13)$$

The HIGGS dataset (Baldi et al., 2014) contains $n = 11,000,000$ observations and 28 covariates. The response is “detected particle” and 21 of the covariates are kinematic properties measured by particle detectors, while 7 are high-level features

to capture non-linearities. The first model we consider for this data is a linear model (in logit scale) \mathcal{M}_1 , which excludes high-level features and has 21 covariates. The second model is a non-linear model (in logit scale) \mathcal{M}_2 , which contains the original covariates and the high-level features, i.e. 28 covariates in total.

The bankruptcy dataset contains $n = 4,748,089$ observations with firm default as the response variable and eight firm-specific and macroeconomic covariates, which gives 9 covariates after adding an intercept. The first model we consider for this data is a linear model (in logit scale) \mathcal{M}_1 with 9 covariates. The second model is a non-linear (in logit scale) bankruptcy model using B -splines as in Dang et al. (2017), with a total of 81 covariates. Nonlinear bankruptcy models for this dataset have been analyzed in Quiroz and Villani (2013) and Giordani et al. (2014).

4.2 Model selection

For both datasets, we are interested in selecting between the linear model \mathcal{M}_1 and the non-linear model \mathcal{M}_2 . Let $\Pr(\mathcal{M}_a)$ denote the prior probability of model a with, $a = 1, 2$. Then the posterior probability of model \mathcal{M}_a is

$$\Pr(\mathcal{M}_a|\mathbf{y}) \propto p(\mathbf{y}|\mathcal{M}_a) \Pr(\mathcal{M}_a),$$

where $p(\mathbf{y}|\mathcal{M}_a)$ is the marginal likelihood of model \mathcal{M}_a . We estimate $p(\mathbf{y}|\mathcal{M}_a)$ with the method outlined in Section 3.5. Given the marginal likelihood of each model, we can compute the Bayes Factor (BF) for a non-linear model \mathcal{M}_2 vs a linear model \mathcal{M}_1 as

$$\text{BF}_{21} = \frac{\Pr(\mathcal{M}_2|\mathbf{y})}{\Pr(\mathcal{M}_1|\mathbf{y})}. \quad (14)$$

A non-linear model is favored if $\text{BF}_{21} > 1$. We use the strength of evidence in Jeffreys (1961, p. 438), in which $10^{3/2} < \text{BF}_{21} < 10^2$ is considered very strong evidence and $\text{BF}_{21} > 10^2$ is decisive evidence. We use the uniform prior $\Pr(\mathcal{M}_1) = \Pr(\mathcal{M}_2) = 1/2$.

4.3 Experimental settings

We compare the performance of our Subsampling SMC against the Subsampling MCMC approach as in Quiroz et al. (2018) and Dang et al. (2017). We note at the outset that it is not possible to compare Subsampling SMC against standard (using all the data) SMC because the latter is computationally infeasible. This is because the full dataset needs to be available at each worker (we use 28) in order to compute the likelihood together with its gradient and Hessian, which quickly consumes the RAM of the computer.

We use the following experimental settings. For both datasets, we use 10 independent runs where each run produces 140 particles distributed among 28 workers to utilize computer parallelism. The 10 separate runs are used to estimate the standard error of the log-marginal likelihood estimates. Moreover, for both datasets, we set $ESS_{\text{target}} = 0.8M$, the number of leapfrog steps $L = 10$, and the number of Markov moves $R = 10$. One may also set R adaptively as in Drovandi and Pettitt (2011), who propose to select R such that there is a high probability that the particle moves at least once. This is particularly important when the proposal of the kernel may have small acceptance probabilities for some region of the parameter space, in which case it is important to set R large when such a region is explored. However, we use HMC which, by the energy conservation property explained in Section 3.4, maintains a high acceptance probability throughout the parameter space. Moreover, we tune HMC to achieve an acceptance probability of approximately 0.8 (see Section 3.4) and therefore $R = 10$ ensures a high probability of moving the particle without the need of adaptation. In Step 1 of Algorithm 1, we let the number of blocks $G = 1,000$ and $G = 100$ and set the subsample sizes $m = 10,000$ and $m = 3000$, respectively, for the HIGGS and bankruptcy datasets.

The same values of m , G and L used by Subsampling SMC are used when implementing Subsampling MCMC. The estimates from the Subsampling MCMC is considered as the “gold standard” when we assess the accuracy of our algorithm. This is achieved through an MCMC chain of 10,000 iterates with another 1,000 iterates discarded as a burn-in period. We have confirmed that all the chains mix well and the iterates are therefore an adequate representation of the true posterior.

4.4 Results

Table 1 shows the estimates of the log marginal likelihood for both models and datasets and the corresponding Bayes factors obtained by Subsampling SMC. The table shows decisively that the non-linear models are superior for both datasets. We again stress that producing marginal likelihood estimates is very convenient by SMC. In fact, in a subsampling context, it is not possible to estimate the marginal likelihood for Subsampling MCMC using common methods such as Chib and Jeliazkov (2001), because the (perturbed) likelihood of Subsampling MCMC cannot be evaluated. This is a major advantage of Subsampling SMC compared to Subsampling MCMC.

Figures 1 and 2 show the kernel density estimates of the marginal posterior of selected parameters of the non-linear model for the HIGGS and bankruptcy datasets. It is evident that Subsampling SMC is very accurate and we have confirmed the accuracy of the kernel density estimates for all the parameters, which we do not show

Table 1: Estimates of the log marginal likelihoods and Bayes factors BF_{21} in (14) for selecting between \mathcal{M}_1 and \mathcal{M}_2 for both datasets. The estimates of the Standard Error (SE) for the marginal likelihood estimates are in parenthesis. The SE is computed using the 10 independent parallel runs. The prior probabilities are $\Pr(\mathcal{M}_1) = \Pr(\mathcal{M}_2) = 1/2$.

	$\log \widehat{p}(\mathbf{y} \mathcal{M}_1)$	$\log \widehat{p}(\mathbf{y} \mathcal{M}_2)$	BF_{21}
HIGGS	-7443136.51 (22.41)	-7014409.33 (22.29)	$\exp(428726)$
Bankruptcy	-214248.28 (106.63)	-205361.10 (54.87)	$\exp(8887)$

here to save space. Instead, Figures 3 and 4 show the estimated marginal posterior expectations and posterior variances by the two algorithms for all the parameters in the non-linear models. This confirms the accuracy of the estimates of each single parameter. We have confirmed that the kernel density estimates and the estimated marginal posterior expectations and posterior variances are accurate also for the linear model (not shown here). Table 2 shows the average (over the 10 independent runs) length of the sequence P for both models and both datasets.

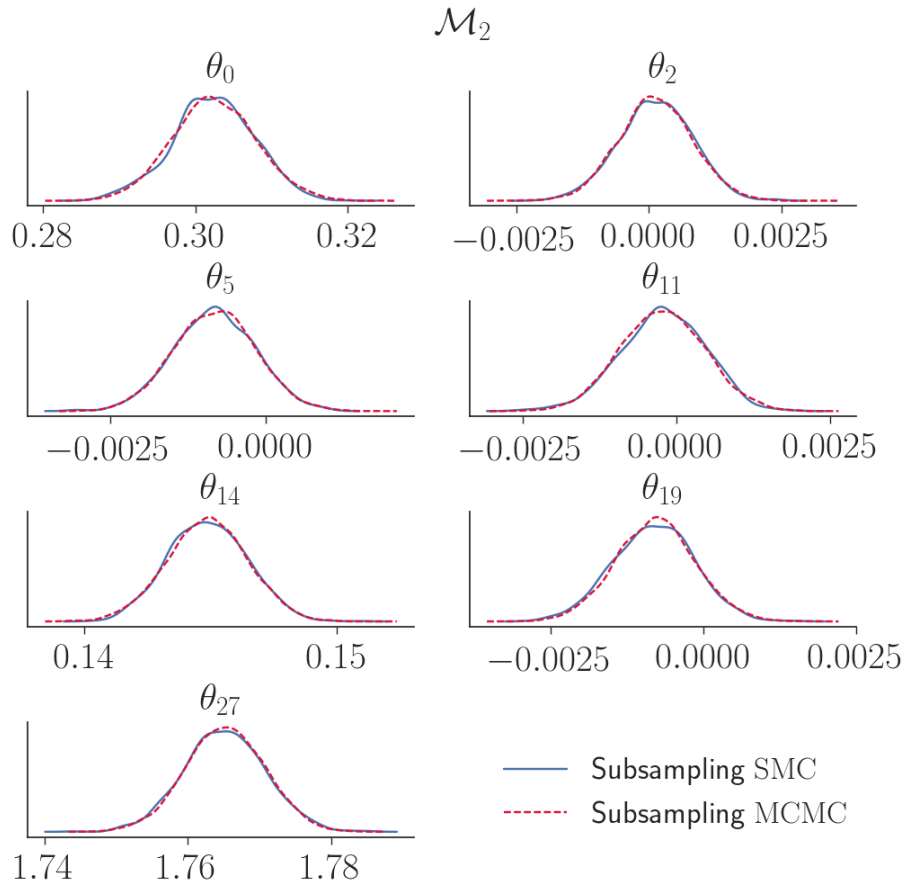


Figure 1: Kernel density estimates of a subset of the marginal posterior densities of θ for the logistic model \mathcal{M}_2 for the HIGGS dataset. The density estimates are obtained by Subsampling MCMC and Subsampling SMC.

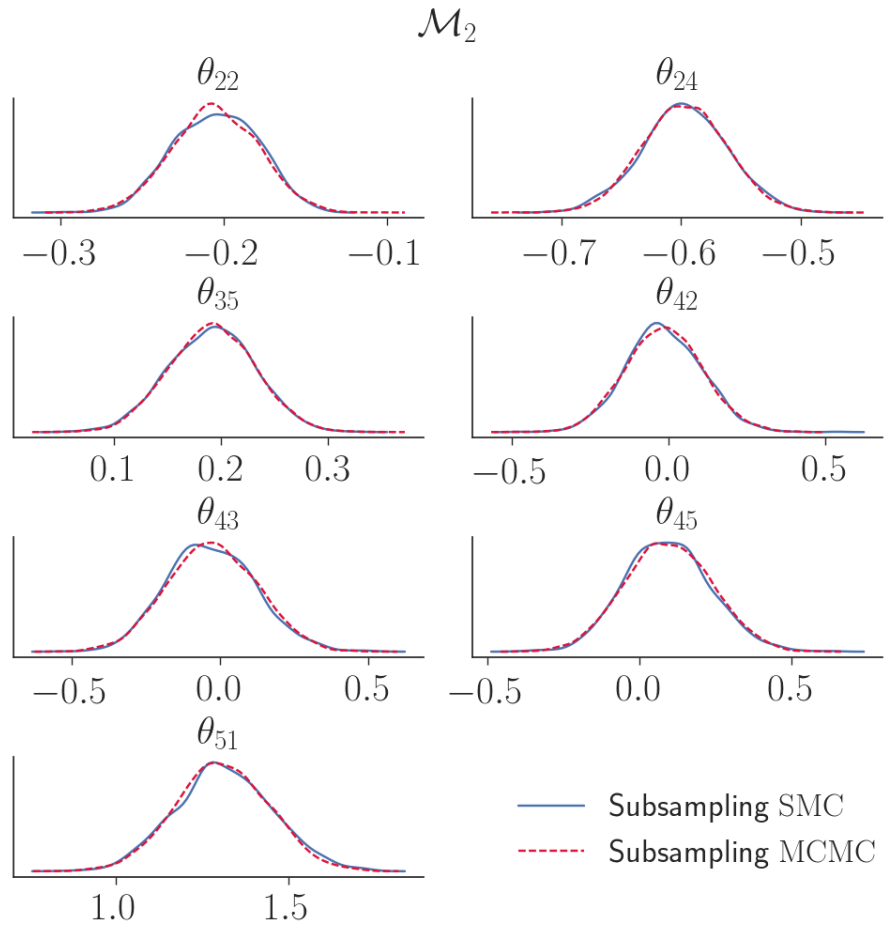


Figure 2: Kernel density estimates of a subset of the marginal posterior densities of θ for the logistic model \mathcal{M}_2 for the bankruptcy dataset. The density estimates are obtained by Subsampling MCMC and Subsampling SMC.

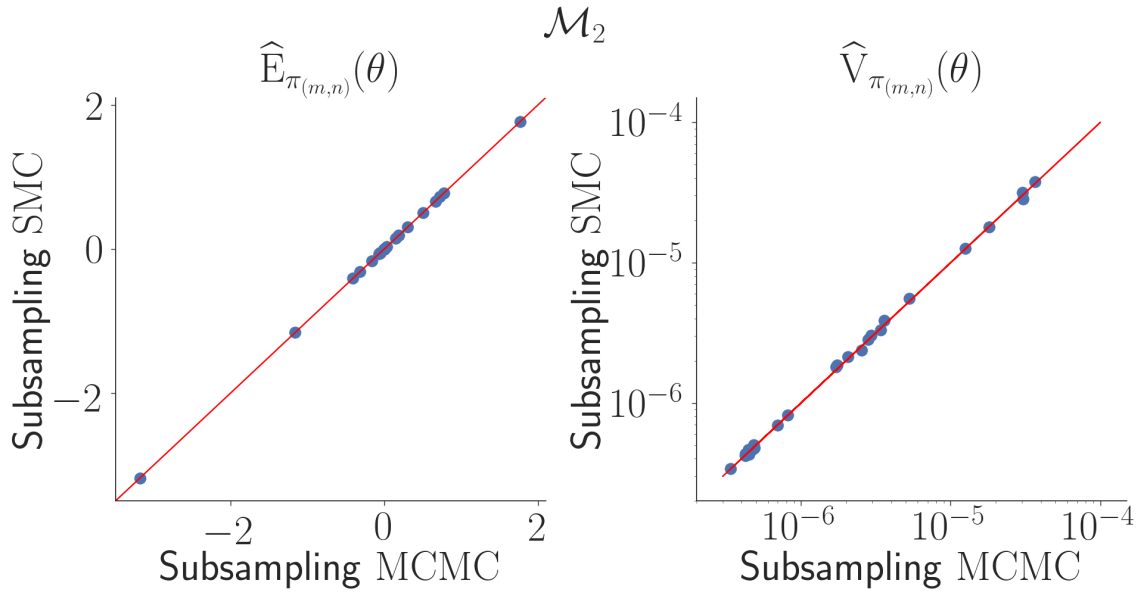


Figure 3: Estimates of marginal means (left panel) and variances (right panel) of θ for the logistic model \mathcal{M}_2 for the HIGGS dataset. The estimates are obtained by Subsampling MCMC and Subsampling SMC and plotted as dots, together with a 45 degree line. This line corresponds to estimates that are in perfect agreement.

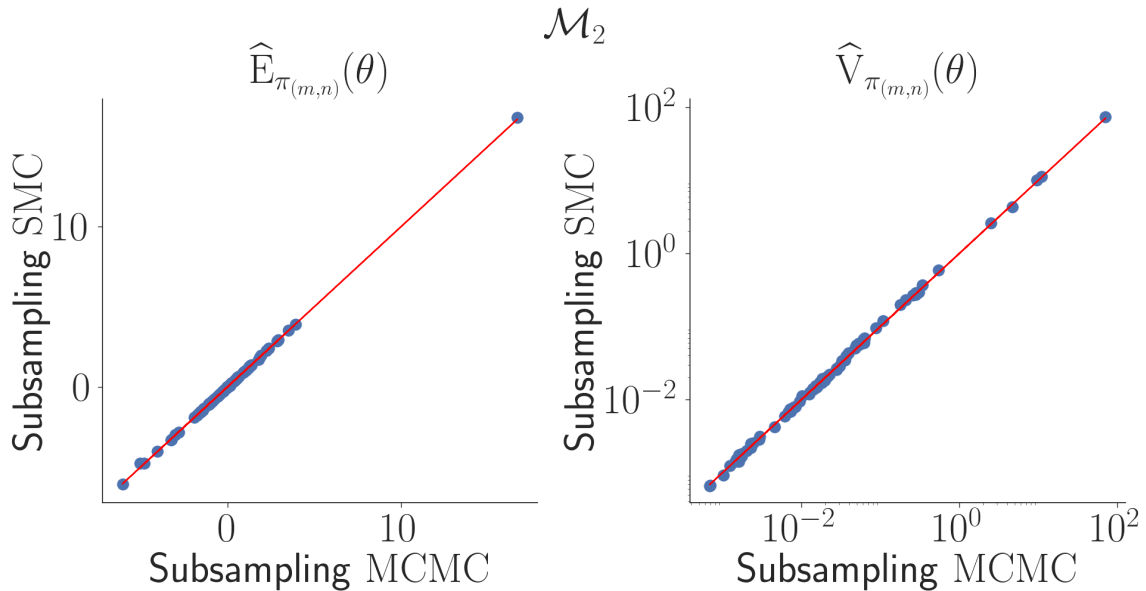


Figure 4: Estimates of marginal posterior means (left panel) and posterior variances (right panel) of θ for the logistic model \mathcal{M}_2 for the bankruptcy dataset. The estimates are obtained by Subsampling MCMC and Subsampling SMC and plotted as dots, together with a 45 degree line. This line corresponds to estimates that are in perfect agreement.

Finally, the superiority of the non-linear model is well understood for the bankruptcy data from Figure 5, which shows that the relationship between the bankruptcy prob-

Table 2: The table shows, for all combinations of datasets and models, \bar{P} which is the average number of sequences lengths P across the 10 independent runs. The algorithm uses the number of leapfrog steps $L = 10$ and the number of Markov moves $R = 10$.

	\mathcal{M}_1	\mathcal{M}_2
HIGGS	120.40	126.80
Bankruptcy	222.80	257.60

ability and the covariate Size is not a logistic function of the covariate as the linear model suggests. The figure shows again that the results obtained from Subsampling SMC are indistinguishable from those of Subsampling MCMC.

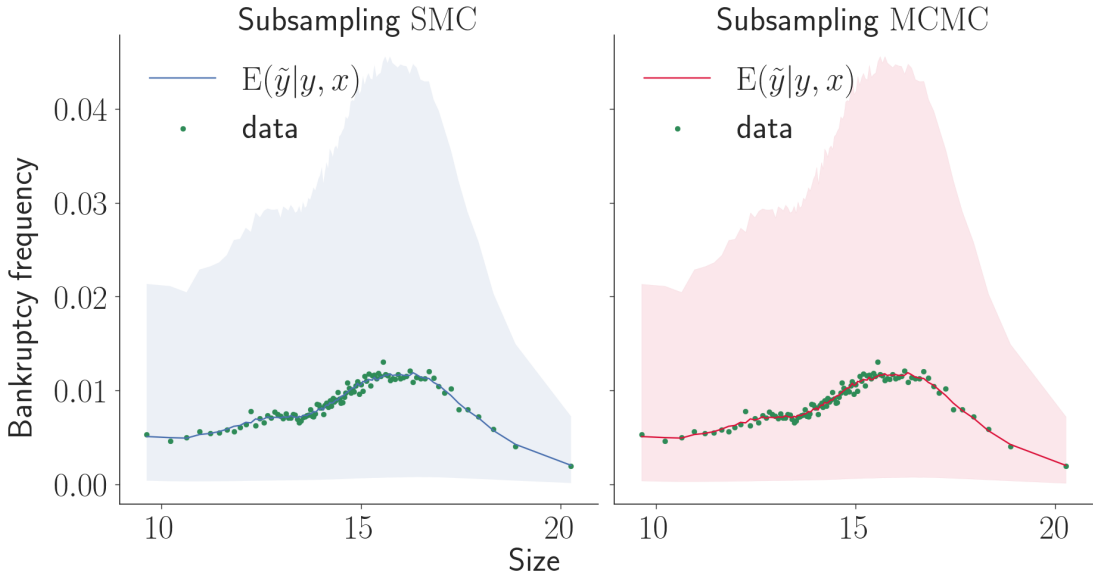


Figure 5: Realized and estimated bankruptcy probabilities. The figure shows the results with respect to the size variable (logarithm of deflated sales) for Subsampling SMC (left panel) and Subsampling MCMC (right panel). The data are divided into 100 equally sized groups based on the size variable. For each group, the empirical estimate of the bankruptcy probability is the fraction of bankrupt firms. These empirical estimates are represented as dots, where the corresponding x -value (size) has been set to the mean within the group. The model estimates for each of the 100 groups are obtained by, for each posterior sample θ , averaging the posterior predictive $\Pr(\tilde{y}_k = 1|\mathbf{y}, x_k)$ for all observations k in a group, and subsequently computing the posterior predictive mean $\mathbb{E}(\tilde{y}_k = 1|\mathbf{y}, x_k)$ (solid line) and 90% prediction interval (quantiles 5-95, shaded region).

5 Conclusions

We propose a simple and effective approach to speed up sequential Monte Carlo for static Bayesian models using data subsampling. The key ingredients of our approach are an efficient annealed likelihood estimator and an effective Markov Kernel move based on Hamiltonian Monte Carlo which boosts particle diversity. This kernel is computationally expensive for large datasets and data subsampling is crucial to obtain a feasible approach. We argue that the subsampling approach is also very convenient for managing computer memory when implementing SMC using parallel computing, because it avoids the need for each worker to store the full dataset. We demonstrate that the method performs efficient and accurate inference on two large datasets and, moreover, that it allows for efficient Bayesian model selection through accurate estimates of the marginal likelihood. This is a major advantage compared to its competitor Subsampling MCMC.

Acknowledgements

David Gunawan, Robert Kohn and Matias Quiroz were partially supported by Australian Research Council Center of Excellence grant CE140100049.

References

- Baldi, P., Sadowski, P., and Whiteson, D. (2014). Searching for exotic particle in high energy physics with deep learning. *Nature Communications*, 5.
- Bardenet, R., Doucet, A., and Holmes, C. (2017). On Markov chain Monte Carlo methods for tall data. *The Journal of Machine Learning Research*, 18(1):1515–1557.
- Beskos, A., Jasra, A., Kantas, N., and Thiery, A. (2016). On the convergence of adaptive sequential Monte Carlo methods. *The Annals of Applied Probability*, 26(2):1111–1146.
- Betancourt, M. (2017). A conceptual introduction to Hamiltonian Monte Carlo. *arXiv preprint arXiv:1701.02434*.
- Brooks, S., Gelman, A., Jones, G., and Meng, X.-L. (2011). *Handbook of Markov chain Monte Carlo*. CRC press.
- Chib, S. and Jeliazkov, I. (2001). Marginal likelihood from the Metropolis-Hastings output. *Journal of American Statistical Association*, 96(453):270–281.

- Chopin, N. (2002). A sequential particle filter method for static models. *Biometrika*, 89(3):539–552.
- Dang, K. D., Quiroz, M., Kohn, R., Tran, M. N., and Villani, M. (2017). Hamiltonian Monte Carlo with energy conserving subsampling. *arXiv preprint arXiv:1708.00955v1*.
- Daviet, R. (2016). Inference with Hamiltonian sequential Monte Carlo simulators. <http://www.remidaviet.com/files/HSMC-paper.pdf>. [Online; accessed 1-May-2018].
- Dean, J. and Ghemawat, S. (2008). MapReduce: simplified data processing on large clusters. *Communications of the ACM*, 51(1):107–113.
- Del Moral, P., Doucet, A., and Jasra, A. (2006). Sequential Monte Carlo samplers. *Journal of the Royal Statistical Society, Series B*, 68:411–436.
- Del Moral, P., Doucet, A., and Jasra, A. (2012). An adaptive Sequential Monte Carlo for approximate Bayesian computation. *Statistics and Computing*, pages 1009–1020.
- Deligiannidis, G., Doucet, A., and Pitt, M. K. (2017). The correlated pseudo-marginal methods. *arXiv preprint arXiv:1511.04992v4*.
- Doucet, A., De Freitas, N., and Gordon, N. (2001). An introduction to sequential Monte Carlo methods. In *Sequential Monte Carlo methods in practice*, pages 3–14. Springer.
- Drovandi, C. C. and Pettitt, A. N. (2011). Using approximate Bayesian computation to estimate transmission rates of nosocomial pathogens. *Statistical Communications in Infectious Diseases*, 3(1).
- Duan, J. C. and Fulop, A. (2015). Density-tempered marginalised sequential Monte Carlo samplers. *Journal of Business and Economics Statistics*, 33(2):192–202.
- Duane, S., Kennedy, A. D., Pendleton, B. J., and Roweth, D. (1987). Hybrid Monte Carlo. *Physics Letters B*, 195(2):216–222.
- Fearnhead, P. and Taylor, B. M. (2013). An adaptive sequential Monte Carlo sampler. *Bayesian Analysis*, 8(2):411–438.
- Garthwaite, P. H., Fan, Y., and Sisson, S. A. (2015). Adaptive optimal scaling of Metropolis-Hastings algorithms using the Robbins-Monro process. *Communications in Statistics - Theory and Methods*.

- Gilks, W. R. and Berzuini, C. (2001). Following a moving target—Monte Carlo inference for dynamic Bayesian models. *Journal of the Royal Statistical Society: Series B (Statistical Methodology)*, 63(1):127–146.
- Giordani, P., Jacobson, T., Von Schedvin, E., and Villani, M. (2014). Taking the twists into account: Predicting firm bankruptcy risk with splines of financial ratios. *Journal of Financial and Quantitative Analysis*, 49(4):1071–1099.
- Gunawan, D., Tran, M.-N., and Kohn, R. (2017). Fast inference for intractable likelihood problems using variational Bayes. *arXiv preprint arXiv:1705.06679*.
- Jasra, A., Stephens, D. A., Doucet, A., and Tsagaris, T. (2011). Inference for Lévy-driven stochastic volatility models via adaptive Sequential Monte Carlo. *Scandinavian Journal of Statistics*, 38(1):1–22.
- Jeffreys, H. (1961). *The Theory of Probability*. OUP Oxford.
- Johnson, A. A., Jones, G. L., and Neath, R. C. (2013). Component-wise Markov chain Monte Carlo: Uniform and geometric ergodicity under mixing and composition. *Statistical Science*, 28(3):360–375.
- Kass, R. E. and Raftery, A. E. (1995). Bayes factors. *Journal of American Statistical Association*, 90(430):773–795.
- Liu, J. S. (2001). *Monte Carlo strategies in scientific computing*. New York: Springer.
- Liu, J. S. and Chen, R. (1998). Sequential Monte Carlo methods for dynamic systems. *Journal of the American Statistical Association*, 93(443):1032–1044.
- Neal, R. (2001). Annealed importance sampling. *Statistics and Computing*, 11:125–139.
- Neal, R. M. (1996). *Bayesian Learning for Neural Networks*. Springer, Lecture Notes in Statistics, New York.
- Neal, R. M. (2011). MCMC using Hamiltonian dynamics. *Handbook of Markov chain Monte Carlo*.
- Quiroz, M., Kohn, R., Villani, M., and Tran, M. N. (2018). Speeding up MCMC by efficient data subsampling. *Journal of American Statistical Association*, To appear.
- Quiroz, M. and Villani, M. (2013). Dynamic mixture-of-experts models for longitudinal and discrete-time survival data. <https://github.com/mattiasvillani/Papers/raw/master/DynamicMixture.pdf>. [Online; accessed 2-May-2018].

- Roberts, G. O. and Stramer, O. (2002). Langevin diffusions and Metropolis-Hastings algorithms. *Methodology and Computing in Applied Probability*, 4(4):337–357.
- Sim, A., Filippi, S., and Stumpf, M. P. (2012). Information geometry and sequential Monte Carlo. *arXiv preprint arXiv:1212.0764*.
- South, L. F., Pettitt, A. N., and Drovandi, C. C. (2016). Sequential Monte Carlo for static Bayesian models with independent MCMC proposals.
- South, L. F., Pettitt, A. N., Friel, N., and Drovandi, C. C. (2017). Efficient use of derivative information within SMC methods for static Bayesian Models.
- Tran, M. N., Kohn, R., Quiroz, M., and Villani, M. (2017). The block-pseudo marginal sampler. *preprint arXiv:1603.02485v5*.